University of Birjand

Water Harvesting Research (2026) Vol. 9, No. 1: 113-123

10.22077/jwhr.2026.11491.1206

ORIGINAL ARTICLE

Evaluation of Bias Correction Methods for CMIP6 Precipitation Projection: A Case Study of Torqabeh City, Iran

Bahareh Sadat Hamraz [a], **Abolfazl Akbarpour** [b*], **Mohammad Hosein Najafimood** [a]

[a]Department of Water Engineering, University of Birjand, Birjand, Iran
[b]Department of Civil Engineering, University of Birjand, Birjand, Iran

*Corresponding Author E-mail Address: akbarpour@birjand.ac.ir

Received: 09 June 2026, **Revised**: 27 June 2026, **Accepted**: 24 July 2026

Abstract

Investigating climate change's impact on precipitation patterns using GCMs is crucial, but correcting their inherent biases is essential for reliable regional applications. The present study aimed to investigate the effect of seven bias correction methods and a weighted ensemble of the five best-corrected models on the accuracy of 14 CMIP6 models in predicting precipitation. Bias correction was performed for the baseline period 1990–2014, and the corrected outputs were validated against observational data from nine meteorological stations using RMSE, PBIAS, KGE, and NSE metrics. Based on the results, the ensemble method was selected as the superior approach at all stations, improving KGE from 0.54 to 0.56 (3.7%), improving NSE from 0.19 to 0.42 (121%), and reducing RMSE from 23.48 to 19.79 (15.7%). The ensemble reduced PBIAS at six stations (by ~77% on average. A one-tailed Wilcoxon signed-rank test confirmed that the superiority of the ensemble method is statistically significant (W = 45, n = 9, p = 0.0039). Among the individual methods, the Bernoulli gamma method, which is based on the separation of dry and wet days and the use of the gamma distribution, had the best performance. In the ensemble method, CESM2, CNRM-CM6-1, and MRI-ESM2-0 were consistently among the top five models at all stations. Precipitation projection using the optimal bias correction method (ensemble) and the best-performing CMIP6 model for the 2030–2055 period indicates that precipitation will decrease by an average of 10.46% under SSP1-2.6 (ranging from -6.1% to –13.7% across stations) and by an average of 14.6% under SSP5-8.5 (ranging from -9.2% to –18.7%).

Keywords: Bernoulli-Gamma, Ensemble, KGE, SSP scenarios, Wilcoxon

1. Introduction

Global climate change has a strong impact on both precipitation patterns and water availability (Mukherjee et al. 2018). General Circulation Models (GCMs) are key tools for understanding and forecasting future climate conditions. Nevertheless, their outputs are inherently biased and subject to substantial uncertainty (Khan et al. 2018). According to Liu et al. (2014), models that account for seasonal variations, geographic characteristics, and topographic conditions yield more reliable projections. With the release of the CMIP6 dataset—currently the most advanced suite of climate simulations—expectations for enhanced model accuracy have grown (Rivera and Arnould 2020). Focusing on Iran, several investigations have already utilized CMIP6 model outputs (Azad and Ahmadi 2025; Zarrin and Dadashi-Roudbari 2021; Zareian et al. 2023; Yazdandoost et al. 2021).

A basic problem in climate modeling is that raw GCM outputs don't work well for local-scale applications. The main reason is systematic mismatches caused by differences in spatial resolution and how physical processes are represented. To overcome this issue, downscaling techniques have been developed, which transform low-resolution GCM predictions into more detailed and regionally relevant projections. These techniques fall into two broad classes: dynamical downscaling, which operates through high-resolution regional climate models, and statistical downscaling, which adjusts model outputs using empirically derived relationships (Chervenkov and Spiridonov 2019). Bias correction (BC) is a specific type of statistical downscaling. It adjusts GCM outputs to match observed records, which improves the accuracy of climate projections (Nguyen et al. 2023).

Over the years, several BC methods have been proposed, including Quantile Mapping (QM), Power Transformation, Empirical Quantile Mapping (EQM), and Linear Scaling, each with its own advantages and limitations. Numerous studies have evaluated these techniques. Gebru et al. (2024) found that Statistical Downscaling Method (SDM), Quantile Delta Mapping (QDM), and QDM95 improved pattern correlations and Taylor skill scores for daily precipitation in South Africa. Spor et al. (2026) applied QM and EQM to bias-correct CMIP6 precipitation outputs in the semi-arid GAP region of Turkey, reporting a marked decrease in projected precipitation under the SSP5-8.5 scenario. Nemati Shishehgaran et al. (2024) showed that, for the Rafsanjan region of Iran, the MPI-ESM1-2-LR model combined with the bernlnorm bias correction technique performed best in simulating precipitation. Song and Chung (2025) demonstrated that, across six continents, EQM yielded the best performance for Southwest Asia, including areas over Iran.

Instead of relying on a single GCM with its own limitations, the multi-model ensemble (MME) approach combines outputs from different models. This helps reduce uncertainties coming from model parameters and structure. Yılmaz et al. (2024) developed four MME approaches with QDM bias correction using six CMIP6 GCMs and projected that precipitation could decrease by up to 43% in the Altınkaya Dam Basin by 2100 under SSP5-8.5. Employing multiple ensemble approaches, Yang et al. (2023) compared an all-model ensemble, a best-model ensemble, and a worst-model ensemble based on 20 CMIP6 models over northern China, demonstrating that the best-model ensemble outperformed the others in simulating winter circulations and projected larger precipitation increases under SSP5-8.5.

Although these methods are widely used, there is no agreement on a single best method that works everywhere. Their performance depends on local climate conditions and which variable is being corrected (Ali et al. 2025). Consequently, a systematic comparison of different bias correction strategies and their optimal combinations for precipitation forecasting have remained relatively scarce.

For this purpose**,** this research aimed to evaluate the performance of 14 selected CMIP6 models in simulating precipitation to determine the appropriate model and to examine and compare the efficiency of seven bias correction models in correcting the predicted precipitation of climate models. Finally, by building an ensemble model and comparing it with individual models, future precipitation projections under two scenarios (SSP1-2.6 and SSP5-8.5) were performed using the optimal model and the most effective bias correction technique .This comparative framework is applied to Torqabeh, Iran – a city characterized by a tourist-based economy and intensive horticulture (notably orchards) – where precipitation variability poses direct risks to both water availability and local livelihoods.

2. Materials and Methods

2.1. Study area

Torqabeh covers an area of 359.25 km² and is located within the UTM coordinate system (Zone 40), with easting coordinates ranging from 685,152 to 733,646 and northing coordinates ranging from 4,002,383 to 4,043,966. This basin is closed on the Jagharg River, which is situated to the west of the second-order Qareh Qom catchment and Mashhad catchment in northeastern Iran. Surface runoff originating from the northern slopes of the Binalud Mountains converges to form the Torqabeh and Shandiz Rivers, which subsequently join the Kashafrud River. The meteorological stations selected for extracting precipitation data are presented in Table 1. All stations share a common statistical period from 1990 to 2014. The selected network, comprising interior and peripheral stations, adequately represents the spatial variability of precipitation across the study area.

The geographical location of the study area is illustrated in Fig. 1.

2.2. CMIP6 models

To investigate the effects of global climate change, the outputs of 14 Atmosphere–Ocean General Circulation Models (AOGCMs) from the Sixth Assessment Report (AR6) of the Intergovernmental Panel on Climate Change (IPCC) were employed, as listed in Table 2. These data were extracted from the Copernicus Climate Data Store for two Shared Socioeconomic Pathway (SSP) scenarios—SSP1-2.6 (optimistic) and SSP5-8.5 (pessimistic)—to produce future projections for the period 2030–2055. Historical model data for the baseline period 1990–2014 were also retrieved. The selection of models was carried out to ensure the inclusion of all models that have been previously used in earlier studies.

Table 1. The studied stations

Station	Longitude (Degree)	Latitude (Degree)	Height (m)
Edareh Mashhad	36.31	59.57	1018
Gomakan	36.48	59.16	1440
Hesar Dehbar	36.31	59.41	1251
jaqarq	36.31	59.32	1434
Mashhad	36.27	59.64	999
Moqan	36.14	59.38	1788
Sad Totoq	36.17	59.55	1242
SarAsiab Shandiz	36.40	59.34	1296
Zoshk	36.34	59.20	1832

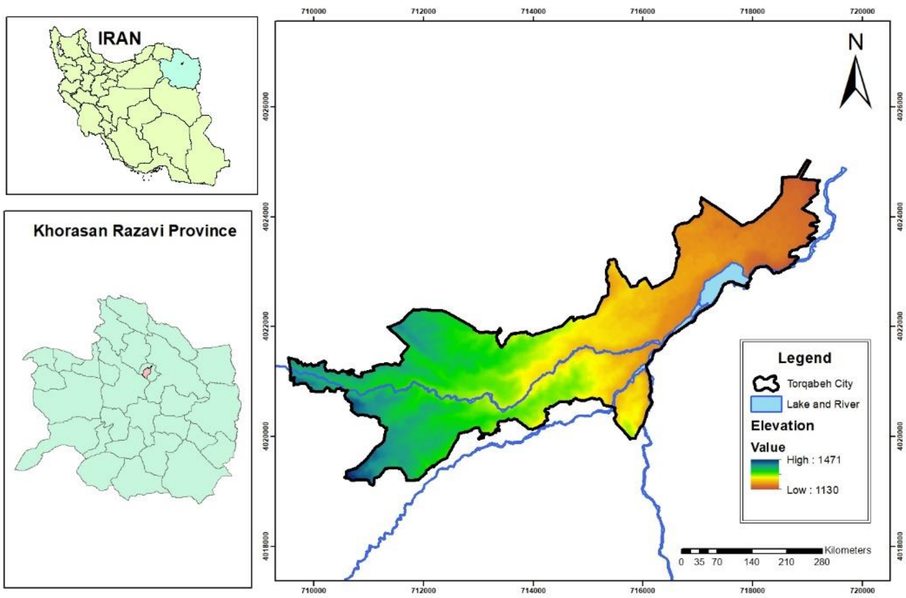

Fig. 1. Geographical location of the study area

Table 2. lists the selected CMIP6 models employed in this study

Model	Institute	Country	Resolution
ACCESS-ESM1-5	Commonwealth Scientific and Industrial Research Organization (CSIRO)	Australia	1.25° x 1.875°
BCC-CSM2-MR	Beijing Climate Center (BCC) China	China	1.12° x 1.125°
CanESM5	Canadian Centre for Climate Modelling and Analysis, Environment and Climate Change Canada (CCCma)	Canada	2.77° x 2.81°
CESM2	National Center for Atmospheric Research, Climate and Global Dynamics Laboratory (NCAR)	USA	0.94° x 1.25°
CMCC-ESM2	Fondazione Centro Euro-Mediterraneo sui Cambiamenti Climatici (CMCC)	Italy	0.94° x 1.25°
CNRM-CM6_1	Centre National de Recherches Meteorologiques (CNRM), Centre Européen de Recherche et de Formation Avancée Calcul Scientifique (CERFACS)	France	1.40° x 1.406°

Model	Institute	Country	Resolution
GFDL-ESM4	National Oceanic and Atmospheric Administration, Geophysical Fluid Dynamics Laboratory (NOAA-GFDL)	USA	1.00° x 1.25°
HadGEM3-GC31_LL	UK Met Office Hadley Centre (MOHC)	UK	1.25° x 1.88°
INM-CM5_0	Institute for Numerical Mathematics, Russian Academy of Science (INM)	Russia	1.50° x 2.00°
MIROC6	Japan Agency for Marine-Earth Science and Technology (JAMSTEC), Atmosphere and Ocean Research Institute, The University of Tokyo (AORI), National Institute for Environmental Studies (NIES),and RIKEN Center for Computational Science (R-CCS, MIROC)	Japan	1.39° x 1.406°
MPI-ESM1-2-LR	Max Planck Institute for Meteorology (MPI-M)	Germany	1.39° x 1.41°
MRI-ESM2-0	Meteorological Research Institute (MRI)	Japan	1.113° x 1.125°
TaiESM1	Research Center for Environmental Changes, Academia Sinica (AS-RCEC)	Taiwan	0.942° x 1.25°
UKESM1-0-LL	UK Met Office Hadley Centre (MOHC)	UK	1.25° x 1.88°

2.3. Bias correction methods

To correct the bias in simulated precipitation values, seven statistical methods were applied, as presented in Table 3. To evaluate the outputs of the models employed in this study, four statistical metrics were used: Root Mean Square Error (RMSE), Percent Bias (PBIAS), Kling-Gupta Efficiency (KGE), and Nash-Sutcliffe Efficiency (NSE). These metrics have been widely applied in previous studies (Enayati et al. 2021; Salman et al. 2020; Song et al. 2020; Khorramnezhad et al. 2024).

To reduce uncertainty in the results obtained from the CMIP6 models, a weighted ensemble of precipitation values was computed for the future period (2030–2055) using the five top-performing AOGCMs. The weights were derived based on the Kling–Gupta Efficiency (KGE) criterion using Eq. 1, in which Wi denotes the weight of each AOGCM model in estimating precipitation.

$$W_i = \frac{KGE_i}{\sum_{j=1}^{n} KGE_j} \tag{1}$$

The Kling–Gupta Efficiency (KGE) decomposes the overall error into three distinct components: correlation (r), variability ratio (α), and mean ratio (β). This decomposition enables a more precise identification of the strengths and weaknesses of each method. Furthermore, it provides a better balance among the different error components.

After evaluating and weighting the models in the previous step, precipitation outputs from various CMIP6 models were extracted for the study area under the two emission scenarios—SSP1-2.6 and SSP5-8.5—for the future period of 2030–2055.

3. Results and Discussion

3.1. Evaluation and ranking of CMIP6 models after bias correction

The performance of the seven bias correction methods was evaluated using the metrics in Table 4. After comparing the bias-corrected GCM outputs against observations, the weighted ensemble of the five top-performing models (based on KGE weights) showed the best performance across all stations.

No single bias correction method worked best at all nine stations .Among the individual methods, berngamma and Empirical Quantile Mapping (EQM) outperformed the others. The berngamma method proved superior at five stations: Golmakan, Jaqarq, Mashhad, Sad Toroq, and Sarasiab Shandiz. Its advantage at these five stations stems from its successful discrimination between dry and wet days. Specifically, it models precipitation occurrence probability using a Bernoulli distribution and precipitation intensity on wet days using a Gamma distribution. The Gamma distribution fits skewed precipitation data well, so berngamma reconstructed heavy events more accurately.

Table 3. Precipitation bias correction methods

Model	Correction Formula	Note	Reference
Linear Scaling	$P_{corr} = P_{model} \times \frac{\mu_{obs}}{\mu_{model}}$	Adjusts mean only	Lafon et al. (2013)
Variance scaling	$P_{corr} = \mu_{obs} + (P_{model} - \mu_{model}) \times \frac{\sigma_{obs}}{\sigma_{model}}$	Adjusts mean & variance	Koutsoyiannis (2006)
Power transformation	$P_{corr} = \alpha \times P_{model}^{b}$ $\alpha = \frac{\mu(p_{obs,d})}{\mu(p_{model,d})}$ b *is found iteratively so that* $\sigma(P_{corr})/\mu(P_{corr}) = \sigma(P_{Obs})/\mu(P_{Obs})$	b is found iteratively	Leander and Buishand (2007)
Empirical Quantile Mapping (EQM)	$P_{corr} = F_{obs}^{-1}(F_{Model}(P_{Model}))$	Non-parametric	Wilcke et al . (2013)
Parametric Quantile Mapping (PQM)	$P_{corr} = F_{Gamma,Obs}^{-1}\left(F_{Gamma,Model}(P_{Model})\right)$	Assumes Gamma distribution	Switanek et al. (2017)
Delta Mapping (QDM)	$\Delta_q = \frac{Q_{model,Futer}(q)}{Q_{model,Hist}(q)}$ $P_{Futer,Corr}(q) = Q_{obs,Hist}(q) \times \Delta_q$	Preserves future relative changes	Cannon et al . (2015)
Bernoulli-Gamma (Berngamma)	$P_{wet,Corr} = P_{wet,Obs}$ $I_{corr} = F_{Gamma.Obse}^{-1}\left(F_{Gamma,Model}(I_{model})\right)$	First corrects wet-day occurrence, then intensity	Piani et al (2010)

The EQM method performed better at two stations: Hesar Dehbar and Zoshk. As a non-parametric method, EQM makes no prior assumptions regarding the data distribution. Its superiority at these two stations suggests that the precipitation distribution in these areas is more complex than can be adequately described by a simple parametric distribution such as the Gamma distribution (even when combined with a Bernoulli component). Extreme skewness, heavy tails, or multi-modality of the precipitation distribution at Hesar Dehbar and Zoshk likely explain the enhanced performance of the flexible EQM approach.

The linear scaling method was selected as the best single method at two stations. However, this method is suitable only for stations with relatively uniform precipitation and no extreme events. For this reason, it is not recommended as a general method for precipitation bias correction.

Among the single-model bias correction approaches, CESM2 exhibited the highest frequency of occurrence as the best-performing individual model, being selected at six out of nine stations (66.7%)

The ensemble method, which combined the five top-performing models using weights derived from the Kling–Gupta Efficiency (KGE) criterion, performed best at all nine stations. The results demonstrate that the ensemble method outperformed the best individual method across all evaluation metrics. Specifically, it improved KGE from 0.54 to 0.56 (3.7%), increased NSE from 0.19 to 0.42 (121%, an absolute increase of 0.23), and reduced RMSE from 23.48 to 19.79 (a reduction of 15.7%). Regarding PBIAS, the ensemble method reduced bias at six stations (by approximately 77% on average) but introduced a small positive bias (ranging from 0.48% to 2.8%) at the three stations where the best individual method had exhibited zero bias. A one-tailed Wilcoxon signed-rank test confirmed that the superiority of the ensemble method is statistically significant ($W = 45$, $n = 9$, $p = 0.0039$).

Table 4. The best bias correction method and the top-ranked CMIP6 model based on error metrics for each station

Station	Method		Models	KGE	NSE	PBIAS	RMSE	Best Method
Edareh Mashhad	linear	Ensemble	CESM2,					
	linear		CNRM_CM6_1					
	linear		MRI_ESM2_0,	0.58	0.46	0	15.46	Ensemble
	linear		BCC_CSM2_MR					
	linear		ACCESS_ESM1_5					
	linear		CESM2	0.56	0.24	0	18.30	
Golmakan	berngamma	Ensemble	CESM2,					
	berngamma		CNRM_CM6_1					
	var_scale		BCC_CSM2_MR	0.58	0.46	-0.1	15.56	Ensemble
	linear		MRI_ESM2_0					
	linear		INM_CM5_0					
	berngamma		CESM2	0.56	0.19	0.57	19.12	
Hesar Dehbar	EQM	Ensemble	TaiESM1,					
	linear		CNRM_CM6_1,					
	linear		MRI_ESM2_0,	0.52	0.36	1.2	17.72	Ensemble
	berngamma		CESM2,					
	linear		ACCESS_ESM1_5					
	EQM		TaiESM1	0.50	0.1	0.0	21.99	
jaqarq	berngamma	Ensemble	CESM2,					
	linear		MRI_ESM2_0					
	linear		CNRM_CM6_1	0.57	0.45	1.36	22.07	Ensemble
	EQM		HadGEM3_GC31_LL					
	linear		BCC_CSM2_MR					
	berngamma		CESM2	0.56	0.18	6.50	26.76	
Mashhad	berngamma	Ensemble	CESM2					
	linear		CNRM_CM6_1					
	linear		MRI_ESM2_0	0.57	0.45	-0.2	17.82	Ensemble
	linear		BCC_CSM2_MR					
	PQM		HadGEM3_GC31_LL					
	berngamma		CESM2	0.56	0.24	-0.58	20.95	
Moqan	linear	Ensemble	CNRM_CM6_1					
	linear		INM_CM5_0					
	linear		MRI_ESM2_0	0.54	0.42	0.48	26.53	Ensemble
	linear		BCC_CSM2_MR					
	berngamma		CESM2					
	linear		CNRM_CM6_1	0.53	0.19	0.0	31.25	
Sad Toroq	berngamma	Ensemble	CESM2,					
	linear		MRI_ESM2_0					
	linear		CNRM_CM6_1	0.56	0.44	0.1	19.12	Ensemble
	EQM		HadGEM3_GC31_LL					
	linear		INM_CM5_0					
	berngamma		CESM2	0.55	0.24	0.57	22.36	
SarAsiab Shandiz	berngamma	Ensemble	CESM2					
	linear		MRI_ESM2_0					
	linear		CNRM_CM6_1	0.6	0.47	0.4	15.99	Ensemble
	EQM		HadGEM3_GC31_LL					
	linear		INM_CM5_0					
	berngamma		CESM2	0.58	0.26	1.68	18.83	
Zoshk	EQM	Ensemble	CMCC_ESM2					
	EQM		HadGEM3_GC31_LL					Ensemble
	berngamma		CESM2	0.52	0.23	2.8	27.92	
	Linear		CNRM_CM6_1					
	Linear		MIROC6					

The ensemble method performed better than any individual method. This confirms that using multiple models reduces uncertainty. According to error theory, averaging reduces total error variance when individual errors are independently distributed with zero mean. Although this ideal condition may not be perfectly satisfied in practice, the substantial improvements observed in KGE and NSE indices are consistent with such variance reduction, reflecting enhanced correlation, reduced error standard deviation, and increased efficiency.

Analysis of the frequency with which climate models appeared among the top five across the nine stations revealed that three models—CESM2, CNRM-CM6-1, and MRI-ESM2-0—were consistently among the top five at all nine stations (100% of cases). These three models are identified as the core of the ensemble. Next, two models—HadGEM3-GC31-LL and BCC-CSM2-MR—were present at six out of nine stations (67%) and are recommended as strong candidates for ensemble inclusion.

Examination of the bias correction methods applied to the five top-performing models showed that linear scaling had the highest frequency of occurrence. Owing to its simplicity and its avoidance of drastic alterations to data structure, linear scaling appears widely in the final ensemble as a "safe" option alongside more complex method. The berngamma method ranked second in terms of frequency.

The ensemble method substantially increases NSE, indicating a large reduction in prediction error variance compared to any individual method. Furthermore, it improves temporal correlation and eliminates the risk of selecting an inappropriate single method.

Regarding PBIAS, the ensemble method reduced the absolute bias by approximately 77% across the six stations where the single model had non-zero bias. However, at three stations (Hesar Dehbar, Moqan, Zoshk) where the single model exhibited zero bias, the ensemble method introduced a small positive bias (0.48–2.8). This trade-off is acceptable given the substantial improvements in other metrics.

These results are consistent with the findings of Nemati Shishehgaran et al. (2024), who also reported that the berngamma method performs best among individual bias correction methods. Both studies emphasize the importance of distinguishing between dry and wet days for precipitation bias correction in arid regions of Iran. However, the present study advances beyond previous work by demonstrating that a KGE-weighted ensemble method can achieve even superior performance.

Comparison with the study by Song and Chung (2025) reveals a discrepancy. Because the study area in the present research is characterized by predominantly dry days, the berngamma method—which explicitly separates dry and wet days using a Gamma distribution—outperformed methods such as EQM in this setting.

3.2. Precipitation projection

Downscaling and projection of precipitation for the period 2030–2055 were conducted for each station under two emission scenarios, SSP1-2.6 and SSP5-8.5, based on the optimal ensemble model selected according to Table 2. Subsequently, bias correction was applied using the ensemble method, and the results are presented graphically in Fig. 2.

As illustrated in Fig. 3, future precipitation projections for each station were generated using bias-corrected and reconstructed data via the Kriging method in ArcGIS 10.8 software. The maps reveal a noticeable reduction in precipitation across the study area under both SSP1-2.6 and SSP5-8.5 scenarios, with the most pronounced decline observed under the pessimistic scenario. The spatial patterns confirm that the study area is expected to experience a general drying trend, consistent with the station-based results presented in Fig. 4.

Analysis of the percentage changes in annual precipitation for the future period relative to the baseline period (1990–2014) reveals that under the optimistic SSP1-2.6 scenario, the range of precipitation reduction varies from 5.3% to 24.1%. To further illustrate the spatial uncertainty inherent in these projections, a boxplot was prepared based on the nine station-scale changes (Fig. 5). This plot shows that 50% of the middle stations (interquartile range) experience precipitation reductions ranging from approximately –6.1% to –13.7% under SSP1-2.6 and from –9.2% to –18.7% under SSP5-8.5, with median values of –7.3% and –10.6%, respectively. These intervals represent the plausible range of expected changes across the region and serve as a quantitative measure of spatial uncertainty, emphasizing that relying solely on a single average value may overlook considerable local variability. Comparison of the two scenarios indicates that Under SSP5-8.5, the average precipitation reduction reaches 14.6% – about 1.4 times higher than under SSP1-2.6 (10.46%). This finding suggests a nonlinear behavior in the response of the regional climate system. The largest precipitation decrease occurs at Zoshk station, with a reduction of 30.9% under the pessimistic scenario.

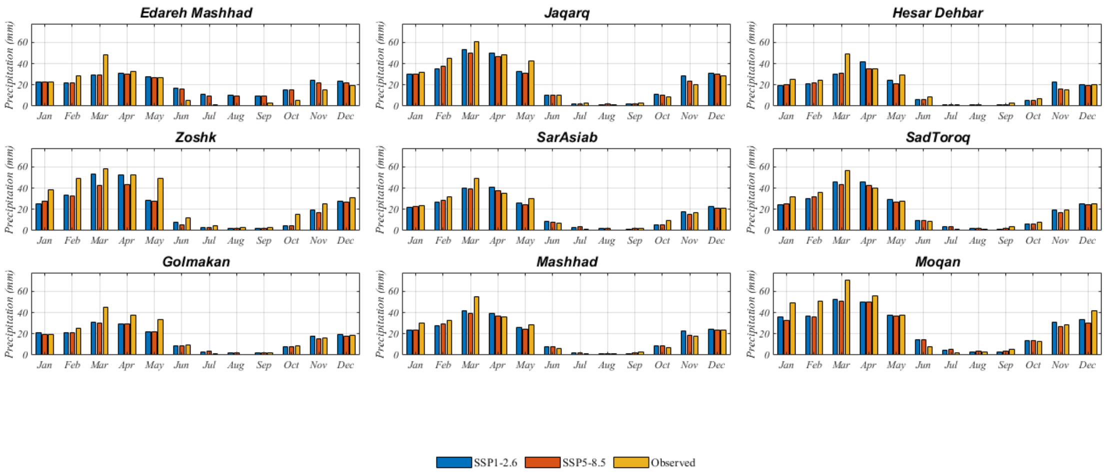

Fig. 2. Precipitation values for emission scenarios by station

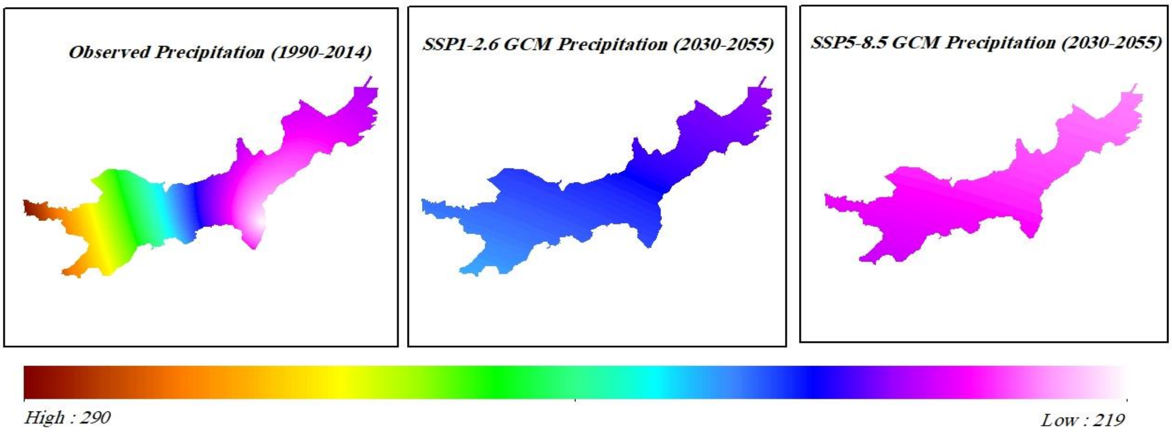

Fig. 3. Spatial patterns of observed and projected annual precipitation (mm) under SSP1-2.6 and SSP5-8.5 scenarios.

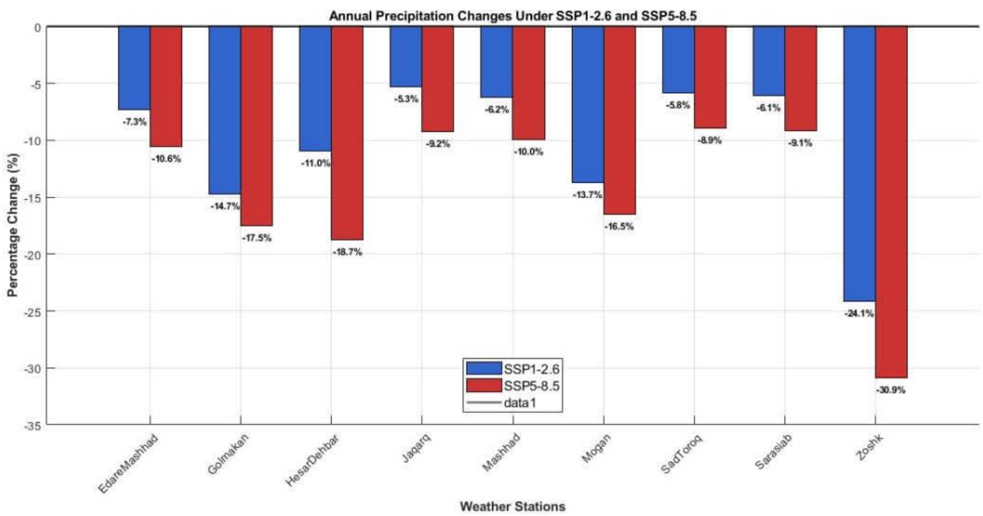

Fig. 4. Percentage changes in annual precipitation in the future period compared to the observational period (1990–2014)

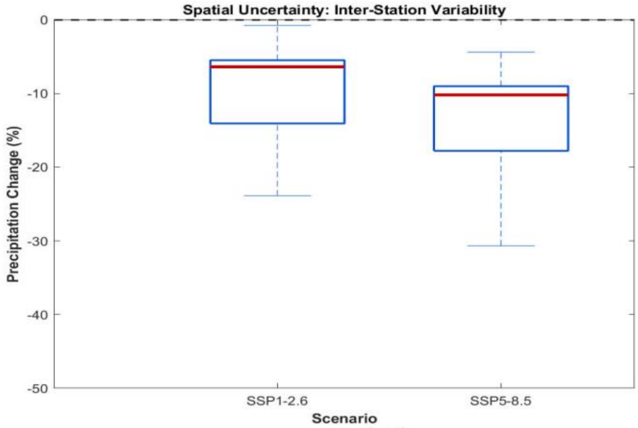

Fig. 5. Spatial uncertainty of projected precipitation changes across stations under SSP1-2.6 and SSP5-8.5

These results are consistent with previous studies in the Kashafrud River basin and Mashhad Plain (where Torghabeh is located), including Doulabian et al. (2021), and Koohi et al. (2020), which projected precipitation reductions ranging from 5% to 15% for similar future periods. A 15% reduction in precipitation in this region is equivalent to the effective loss of one to two months of annual effective precipitation. This decline will reduce aquifer recharge, raise irrigation demand as evapotranspiration increases, and force greater reliance on non-conventional water sources.

3.3. Seasonal changes

To better understand the temporal distribution of future precipitation, changes in seasonal precipitation were also analyzed. The results (Fig. 6) show that precipitation in spring and winter will decrease significantly, which could seriously impact water resources and agriculture. In contrast, summer precipitation shows a percentage increase; however, due to the low absolute amount of summer precipitation, the volumetric increase is only 2 to 3 mm. Therefore, summer will remain the driest season in Iran, even under the optimistic scenario. Autumn precipitation shows mixed behavior, with a slight increase under SSP1-2.6 and a modest decrease under SSP5-8.5, indicating lower confidence compared to other seasons, this finding is consistent with Naderi (2025), but emphasizes that the increase is volumetrically negligible and does not compensate for the substantial reductions expected in the wet seasons.

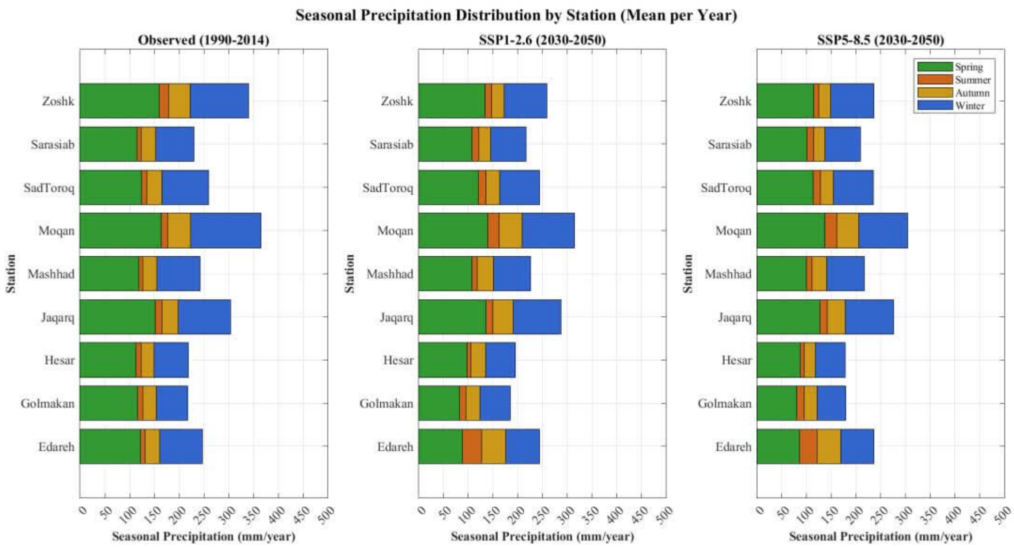

Fig. 6. Seasonal precipitation distribution by station under SSP1-2.6 and SSP5-8.5 scenarios.

Moreover, despite the small volumetric increase, the occurrence of intense summer rainfall events—even with low total amounts—may raise the risk of flash floods, particularly in semi-arid and mountainous catchments such as the Torghabeh region, where short-duration storms can produce rapid runoff.

4. Conclusion

Among the individual bias correction methods, the Bernoulli-gamma (berngamma) method demonstrated the best performance. The EQM and linear scaling methods each achieved the top rank at two stations, but their performance depended strongly on local conditions.

The ensemble method based on KGE weighting—using the five best-corrected models—was selected as the optimal bias correction approach. It improved KGE by 3.7% (from 0.54 to 0.56), increased NSE by 121% (from 0.19 to 0.42), reduced RMSE by 15.7% (from 23.48 to 19.79), and lowered PBIAS by 77%. This method worked especially well for reducing errors in heavy precipitation, which is still the main challenge in precipitation bias correction.

The three models—CESM2, CNRM-CM6-1, and MRI-ESM2-0—were consistently among the top five at all nine stations in the study region. Linear scaling and Bernoulli-gamma were the dominant methods within this ensemble. Therefore, although the Bernoulli-gamma method is suitable for precipitation bias correction in arid and semi-arid regions of Iran, combining multiple top-performing models can further reduce prediction error and uncertainty.

Consistent with the IPCC Sixth Assessment Report scenarios, none of the stations in the study area will experience an increase in precipitation under either future pathway. The average precipitation reduction is projected to be 11.9% under the optimistic scenario (SSP1-2.6) and 14.6% under the pessimistic scenario (SSP5-8.5). The boxplot analysis shows that 50% of the stations exhibit precipitation reductions ranging from –6.1% to –13.7% under SSP1-2.6 and from –9.2% to –18.7% under SSP5-8.5, indicating considerable spatial uncertainty that should be considered in regional impact studies. This reduction is equivalent to losing one to two months of effective annual precipitation in the region and could seriously endanger the sustainability of water-dependent economic activities, including tourism and horticulture.

5. Conflict of interest

No potential conflict of interest was reported by the authors.

6. References

Ali, Z., Muhammad, M. K. I., Almazroui, M., & Shahid, S. (2025). Comparative analysis of bias correction methods for projecting extreme precipitation and temperature indices in Pakistan. *Atmospheric Research,316*,107957. https://doi.org/10.1016/j.atmosres.2025.107957

Azad, N., & Ahmadi, A. (2025). Assessing temperature and precipitation bias nonstationarity of CMIP6 global climate models over Iran. *Theoretical and Applied Climatology, 156*(2), Article 80. https://doi.org/10.1007/s00704-024-05322-w

Chervenkov, H., & Spiridonov, V. (2019). Sensitivity of selected ETCCDI climate indices from the calculation method for projected future climate. In I. Dimov & S. Fidanova (Eds.), *Advances in High Performance Computing: Results of the International Conference on "High Performance Computing" Borovets, Bulgaria, 2019* (pp. 413-427). Springer. https://doi.org/10.1007/978-3-030-55347-0_35

Doulabian, S., Golian, S., Shadmehri Toosi, A., & Murphy, C. (2021). Evaluating the effects of climate change on precipitation and temperature for Iran using RCP scenarios. *Journal of Water and Climate Change, 12*(1), 166-184. https://doi.org/10.2166/wcc.2020.255

Enayati, M., Bozorg-Haddad, O., Bazrafshan, J., Hejabi, S., & Chu, X. (2021). Bias correction capabilities of quantile mapping methods for rainfall and temperature variables. *Journal of Water and Climate Change, 12*(2), 401-419. https://doi.org/10.2166/wcc.2020.261

Gebru, A., Tesfuhuney, W., Motsoane, T., & Rientjes, T. (2024). Improving Daily CMIP6 Precipitation in Southern Africa Through Bias Correction—Part 1: Spatiotemporal Characteristics. *Atmosphere, 15*(12), 1507. https://doi.org/10.3390/atmos15121507

Khan, N., Shahid, S., Ahmed, K., Ismail, T., Nawaz, N., & Son, M. (2018). Performance assessment of general circulation model in simulating daily precipitation and temperature using multiple gridded datasets. *Water, 10*(12), 1793. https://doi.org/10.3390/w10121793

Khorramnezhad, V., Akbarpour, A., & Nazeri Tahroudi, M. (2024). Forecasting and Modeling of Dew Point Temperature in Meteorological Stations of Eastern Region of Iran Based on VAR and VAR-GARCH Models. *Water Harvesting Research*, *7*(1), 34-50. https://doi.org/10.22077/jwhr.2024.7634.1138

Koohi, M., Shirmohammadi-Aliakbarkhani, Z., Mohammadian, A., & Habibi Nokhandan, M. (2020). Study of spatiotemporal distribution of temperature and reference evapotranspiration using CRU data in Khorasan Razavi and projection of future changes based on CMIP5 climate models. *Iranian Journal of Remote Sensing & GIS, 12*(1), 55-72. https://doi.org/10.52547/gisj.12.1.55

Liu, Z., Mehran, A., Phillips, T. J., & AghaKouchak, A. (2014). Seasonal and regional biases in CMIP5 precipitation simulations. *Climate Research, 60*(1), 35-50. https://doi.org/10.3354/cr01221

Mukherjee, S., Aadhar, S., Stone, D., & Mishra, V. (2018). Increase in extreme precipitation events under anthropogenic warming in India. *Weather and Climate Extremes, 20*, 45-53. https://doi.org/10.1016/j.wace.2018.03.005

Naderi, M. (2025). Projections of major climate change indicators over Iran from 2021 to 2080. Environmental Science and Pollution Research, 32(11), 7002–7024. https://doi.org/10.1007/s11356-025-36186-w

Nemati Shishehgaran, N., Babaeian, F., & Mianabadi, H. (2024). Comparison of CMIP6 climate models and quantile mapping bias correction methods in the simulation of precipitation. *Iranian Journal of Soil and Water Research, 55*(6), 1843-1862. https://doi.org/10.22059/ijswr.2023.366061.669585

Nguyen, D. T., Ashraf, S., Le, M., Trung, L. Q., & Ali, M. (2023). Projection of climate variables by general circulation and deep learning model for Lahore, Pakistan. *Ecological Informatics, 75*, 102077. https://doi.org/10.1016/j.ecoinf.2023.102077

Rivera, J. A., & Arnould, G. (2020). Evaluation of the ability of CMIP6 models to simulate precipitation over Southwestern South America: Climatic features and long-term trends (1901–2014). *Atmospheric Research, 241*, 104953. https://doi.org/10.1016/j.atmosres.2020.104953

Salman, S. A., Nashwan, M. S., Ismail, T., & Shahid, S. (2020). Selection of CMIP5 general circulation model outputs of precipitation for peninsular Malaysia. *Hydrology Research, 51*(4), 781-798. https://doi.org/10.2166/nh.2020.154

Song, Y. H., & Chung, E. S. (2025). Inter comparison of bias correction methods for precipitation of multiple GCMs across six continents. *Geoscientific Model Development, 18*(20), 8017-8045. https://doi.org/10.5194/gmd-18-8017-2025

Song, Y. H., Chung, E. S., & Shiru, M. S. (2020). Uncertainty analysis of monthly precipitation in GCMs using multiple bias correction methods under different RCPs. *Sustainability, 12*(18), 7508. https://doi.org/10.3390/su12187508

Spor, P., Aksoy, B., Atalay, C., Kartal, V., & Çıtakoğlu, H. (2026). Hydroclimatic change detection based on observations and bias-corrected CMIP6 projections under SSP scenarios. *Sustainability, 18*(8), 4014. https://doi.org/10.3390/su18084014

Yang, X., Zhou, B., Xu, Y., & Han, Z. (2023). CMIP6 evaluation and projection of precipitation over northern China: further investigation. *Advances in Atmospheric Sciences, 40*(4), 587-600. https://doi.org/10.1007/s00376-022-2150-1

Yazdandoost, F., Moradian, S., Izadi, A., & Aghakouchak, A. (2021). Evaluation of CMIP6 precipitation simulations across different climatic zones: Uncertainty and model intercomparison. *Journal of Hydrology, 603*, Article 126858. https://doi.org/10.1016/j.jhydrol.2021.126858

Yılmaz, B., Aras, E., & Nacar, S. (2024). A CMIP6-ensemble-based evaluation of precipitation and temperature projections. *Theoretical and Applied Climatology, 155*(8), 7377-7401. https://doi.org/10.1007/s00704-024-05073-8

Zareian, M. J., Dehban, H., & Gohari, A. (2023). Evaluation of the accuracy of CMIP6 models in estimating the temperature and precipitation of Iran based on a network analysis. *Water and Irrigation Management, 11*(4), 781-795. https://doi.org/10.22059/jwim.2022.345975.1006

Zarrin, A., & Dadashi-Roudbari, A. (2021). Projection of future extreme precipitation in Iran based on CMIP6 multi-model ensemble. *Theoretical and Applied Climatology, 144*(1-2), 643-660. https://doi.org/10.1007/s00704-021-03568-2